2011 50th IEEE Conference on Decision and Control and
European Control Conference (CDC-ECC)
Orlando, FL, USA, December 12-15, 2011

Parameter Estimation of a Building System Model and Impact of Estimation Error on Closed-Loop Performance

S. Bengea, V. Adetola, K. Kang, M. J. Liba, D. Vrabie, R. Bitmead, S. Narayanan

Abstract— **Predictive-control methods have been recently employed for demand-response control of building and district-level HVAC systems. Such approaches rely on models and parameter estimates to meet comfort constraints and to achieve the theoretical system-efficiency gains. In this paper we present a methodology that establishes achievable targets for control-model parameter estimation errors based on closed-loop performance sensitivity. The control algorithm is designed as a Model Predictive Controller (MPC) that uses perturbed building-model parameters. We perform simulations to estimate the dependency of energy cost and constraint infringement time on the magnitude of these perturbations. The simulation results are used to define targets for the parameter estimation errors, which in turn are applied to specify the character of excitation and model structure used for identification. We design a parameter estimator and perform Monte-Carlo simulations for a model that includes sensor noise and load uncertainty. The distribution of the estimation errors are used to demonstrate that the established targets are met.**

I. Introduction

Building heating and cooling systems consume 12% of total US energy. These systems have received renewed interest from the research community driven by the significant impact that modern design techniques can have as energy prices continue to rise [1]. The challenges in improving their performance dramatically are: unavailability of data due to inadequate instrumentation and/or data communication between systems; complexity of heterogeneous spatially-distributed systems that are installed in districts and campuses; large uncertainties in exogenous factors such as usage, weather; legacy controllers which use local measurements and are re-tuned by operators.

The recent availability of heterogeneous building climate sensors and the capabilities of modern building automation systems overcome the above-mentioned barriers and facilitate the application of system identification and optimal control design techniques for minimizing energy consumption while meeting thermal comfort constraints. These control algorithms can ensure that the energy savings estimated during the design phase persistent over the building lifecycle. The performance of advanced control algorithms depends on the estimation accuracy of the control-model parameters whose knowledge is critical for disturbance rejection with minimum energy consumption. Sensor measurement noise and unmeasured disturbances lead to parameter estimation errors. When bounds on these errors are established earlier in the design phase they can guide the selection of the sensor architecture and estimation technique.

In this paper, we focus on estimating the parameters associated with a building thermal model and develop a methodology for evaluating the impact of parameter estimation errors on closed-loop performance of a selected control design. The model is formulated as a thermal network whose nodes consist of temperature values at different locations in a building. To estimate the sensitivity of the closed-loop performance metrics with respect to the thermal network parameters, we design an MPC algorithm based on perturbed plant model parameters and run various simulation scenarios. Using these simulation results, we establish (i) the critical parameters based on their closed-loop performance impact and (ii) a correspondence between estimation errors and performance metrics that ultimately can be used to select acceptable estimation error bounds. For parameter estimation, we implement several known batch and recursive estimation algorithms (e.g. Finite-Time method, Least Squares variants). To determine if the selected parameter-estimate quality thresholds are met, realistic probability distributions of the estimation errors are generated by Monte-Carlo simulations where the parameter estimation algorithm is subjected to measurement noise and load uncertainty. This ensures that the simulation-based performance criteria are met when the controller is designed with the estimated model parameters.

Experimental excitation signal design and model structure selection are two important *user variables* of system identification and here they are tied to the eventual closed-loop properties of the system when controlled via MPC and feedback linearization. Identified parameter variability is affected by the excitation signal and by the parametrization structure and dimension. This variability is transferred to the closed-loop system in a non-obvious fashion, but is measurable via the sensitivity of the closed-loop performance at the nominal parameter value. This sensitivity is evaluated via simulation.

Building internal spaces have been modeled as thermal networks in a number of papers including [8], [9], [10], [11], [16]. The RC network analogy allows one to conveniently model the temperatures in state-space form that can be used for control [10], load estimation [8], [9], [12], and parameter estimation using techniques such as Least Squares [11]. Alternative modeling approaches include neural networks

This work was supported by United Technologies Research Center (UTRC) and Environmental Security Technology Certification Program (Project EW-0938)

S. Bengea, V. Adetola, K. Kang, D. Vrabie and S. Narayanan are with UTRC, East Hartford, CT 01608, USA {bengeasc, adetolva, kangk, vrabiedl, narayas}@utrc.utc.com

R. Bitmead is with UCSD, rbitmead@ucsd.edu

M. Liba is with Systems and Process Control, Hatch, mliba@hatch.ca

[15] and black-box [17]. The energy savings potential of different control strategies (e.g. rule-based and MPC) for different building types have also been evaluated in [18], [19]. The cited efforts use parameters calculated directly from buildings' architectural construction properties and do not consider the potential impact of parameter estimation errors on the closed-loop performance and comfort constraints infringement.

We focus on an HVAC application where the plant, modeled in Section II, consists of a commercial building area served by a multi-zone HVAC unit. In Section III, we design an MPC algorithm using a control model that is structurally identical to the plant model but has perturbed parameters. We then simulate the closed-loop system and evaluate the impact of the perturbations on energy cost. We regard the temperature constraints as *soft* constraints and instead of designing a robust controller we choose to also evaluate the impact of perturbations on the constraint infringement time. In Section IV we use variants of the Least Squares algorithm to estimate the parameters. Here we also simulate the impact of random sensor measurements and load uncertainties.

II. Plant and Estimation Model Development

In this section, we introduce the state-space models which describe the temperature dynamics in selected spaces of a building. We focus on demand-control applications where the HVAC heat exchangers' supply water flow rate and temperature are controlled in order to meet the requested demand. For this application, the control variables are supply air flow and temperatures to several spaces to meet the demand set through the temperature reference signal. This work focuses on minimizing supplied thermal energy and does not models the efficiencies of the heat exchangers.

The model is a multi-input (thermal energy supplied to multiple zones) and multi-output (temperatures) network whose nodes represent temperature values of entities which are assumed to be isothermal (walls, rooms, zones). The network parameters are directly linked to the time constants associated with the heat transfer from the HVAC unit, adjacent zones, and external, uncontrolled spaces.

Throughout the paper we use the following nomenclature[1]:

- Inputs: $\dot{m}_{sa,S_i}$ and T_{sa,S_i} denote the mass flow rate and temperature of air, respectively, supplied to space S_i; $\dot{m}_{sa}$ denotes the total mass flow rate of the supply air;
- Temperature disturbances: $T_E = [T_{gr,S_i},\ T_{cei,S_i},\ T_{S_{u,i}}]$, where the first two temperatures correspond to ground and ceiling surface in space S_i, and $T_{S_{u,i}}$ is the air temperature of space $S_{u,i}$, illustrated in Fig. 1, whose supply energy is provided by an external source;
- Load disturbances: $Q_{S_i,int}$ represents the overall load in space S_i and consists of heat gains from occupants, lighting, equipment, and convective gains from adjacent spaces; we denote the vector of all space loads as $Q_{S,int}$

[1]The subscripts have the following interpretation: *sa* - supply air; *a* - air; *w* - wall; *gr* - ground; *cei* - ceiling; *int* - internal; *c* and *u* are used to identify spaces where the supply energy is controlled and not controlled, respectively.

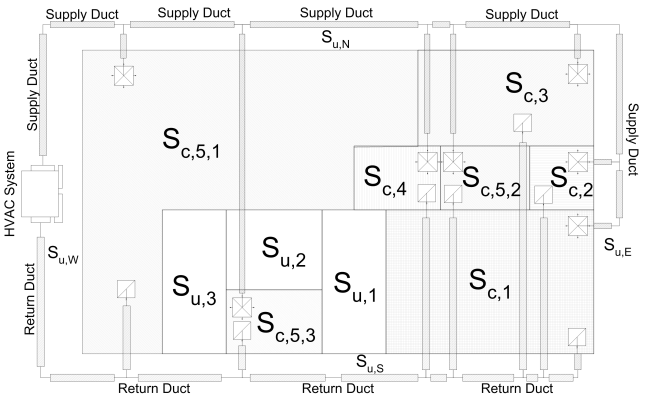

Fig. 1. Selected modeling area layout.

- Dynamical states: $T_{S_{c,i}}$ is air temperature in space $S_{c,i}$ where the supplied energy is generated by a controllable source; T_{w,S_i,S_j} represents the wall-film surface temperature of the wall between spaces S_i and S_j, on the inner surface of space S_i (order of subscripts indicates the space on whose inner surface the temperature is defined);
- Parameters (assumed temperature independent): h_w, h_{gr} and h_{ceil} are the surface-film heat-transfer coefficients per unit area associated with wall, ground and ceiling surfaces (assumed to be uniform in all spaces S_i); R_w and C_w denote the thermal resistance and capacitance per unit area associated with each wall (assumed to be the same for all walls); C_{S_i} is the overall thermal capacitance associated with space S_i;
- Constants: area of the wall, ground and ceiling surfaces: $A_{w,Si,Sj}$, $A_{cei,Si}$, $A_{gr,Si}$; specific heat constant of air C_{pa}; m_{a,S_i} is the air mass in space S_i;.

We model the temperature dynamics in multiple rooms via building thermal network models which are derived under the following standard assumptions ([4], [2]):

A1. All wall properties are assumed to be homogenous with constant thermal conductivity values.

A2. Each surface temperature is assumed to be uniform over the surface it is defined on.

A3. The space air is assumed to be well mixed and the space temperature is assumed to be uniform in the entire space.

In addition we make the following simplifying assumptions:

A4. The latent load is not captured by the models presented in this work.

A5. The solar radiation heat gains are negligible; the selected internal area does not have any external walls.

A6. The mass flow rate of the air supplied to space S_i, $\dot{m}_{sa,S_i}$, is a constant portion of the total supply mass flow rate $\dot{m}_{sa}$. (This is motivated by the particular design of the HVAC unit considered in this work.)

Thermal network models have been traditionally used ([2]) for modeling the heat transfer within building spaces. These models are used in building-design oriented software environments, such as EnergyPlus [13] and TRNSYS [14], and

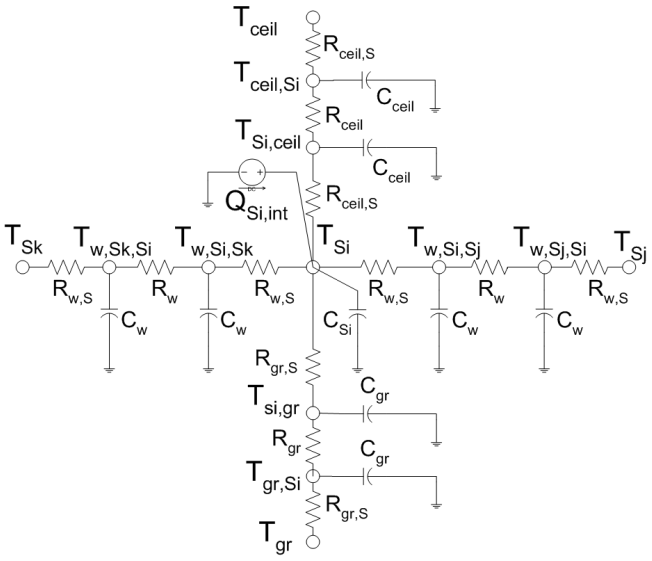

Fig. 2. Electrical circuit representation of the thermal network for space S_i.

are based on direct analogies with electrical circuits. For an area layout illustrated in Fig. 1, we use a two-capacitor-three-resistance-circuit equivalent thermal network, depicted in Fig. 2, to model the internal temperature dynamics. Using the assumptions A2 and A3, the application of the sensible-load-balance equation relates the dynamics of the space air temperature T_{S_i} to the supply mass flow rate $\dot{m}_{sa,S_i}$, supply temperature T_{sa,S_i} and inner wall surface temperatures T_{w,S_i,S_j} as follows:

$$\begin{aligned} C_{S_i}\frac{dT_{S_i}}{dt} &= \dot{m}_{sa,S_i}C_{pa}(T_{sa,S_i}-T_{S_i})+\sum_j \frac{(T_{w,S_i,S_j}-T_{S_i})}{R_{w,S_{i,j}}} \\ &\quad +\frac{(T_{ceil,S_i,S_j}-T_{S_i})}{R_{ceil,S_i}}+\frac{(T_{gr,S_i}-T_{S_i})}{R_{gr,S_i}}+Q_{S_i,int} \end{aligned} \quad (1)$$

where S_j are all the adjacent spaces, $C_{S_i}=m_{a,S_i}C_{pa}$, $R_{gr,S_i}=1/(h_{gr}A_{gr,S_i})$, $R_{ceil,S_i}=1/(h_{ceil}A_{ceil,S_i})$ and $R_{w,S_{i,j}}=1/(h_wA_{S_i,S_j})$. For compactness we have dropped the time argument for the time-varying input and state variables; all parameters are assumed to be time-invariant.

The temperature dynamics of the inner and outer wall surface T_{w,S_i,S_j} and T_{w,S_j,S_i} respectively, between spaces S_i and S_j are described by the following equations:

$$\begin{aligned} C_{w,S_i,S_j}\frac{dT_{w,S_i,S_j}}{dt} &= \frac{(T_{S_i}-T_{w,S_i,S_j})}{R_{w,S_{i,j}}}+\frac{(T_{w,S_j,S_i}-T_{w,S_i,S_j})}{R_{w,S_i,S_j}} \\ C_{w,S_i,S_j}\frac{dT_{w,S_j,S_i}}{dt} &= \frac{(T_{S_j}-T_{w,S_j,S_i})}{R_{w,S_{i,j}}}+\frac{(T_{w,S_i,S_j}-T_{w,S_j,S_i})}{R_{w,S_i,S_j}} \end{aligned} \quad (2)$$

where $C_{w,S_i,S_j}=C_wA_{w,S_i,S_j}$ and $R_{w,S_i,S_j}=\frac{R_w}{A_{w,S_i,S_j}}$. Applying (1) and (2) to all the spaces in the area of Fig. 1, the state-space description of the thermal network model can be written as:

$$\dot{x}=F(x,u)+G(x,T_E)p+Q_{S,int} \quad (3)$$

where: the state $x=[T_{S_i},\ T_{w,S_i,S_j}]$ includes all space and wall surface temperatures; u is the input vector (overall supply flow $\dot{m}_{sa}$ as explained in assumption A6. and individual supply temperatures $\dot{T}_{sa,S_i}$ to each space); p is the vector of unknown parameters, $p=\left[\begin{array}{ccccc} h_w & h_{gr} & h_{cei} & \frac{h_w}{C_w} & \frac{1}{R_wC_w}\end{array}\right]^T$. The components of p are re-defined based on the original parameters in (1) and (2). The new parameters are expressed in this fashion in order to develop a model (3) that is linear with respect to p.

We observe from (1) and (2) that matrix $G(x,T_E)$ is relatively sparse due to the local interdependence of the temperatures T_{S_i} and T_{w,S_i,S_j}. In Section IV, we discuss the effect of this structure on the identifiability of vector p.

The above discussion uses generic space S_i; it is possible that S_i is a room or a set of rooms controlled by the same thermostat (commonly referred to as a *zone*). When each of the spaces S_i of Fig. 1 represents a room R_i, one assigns a temperature state to each room T_{R_i} and applies the same set of equations (1) and (2) to describe each room's dynamics. We call this *room*-level model and we denote its corresponding form (3) as $M_R([T_R,T_W],[u,\ T_E,\ Q_{R,int}],p_R)$ that has air and surface temperatures as states in the rooms and on their wall surfaces. We use model M_R in Section III for MPC design and sensitivity analysis and in Section IV for parameter estimation.

III. Closed-Loop Performance Sensitivity to Parameter Estimation Error

In this section we present the overall approach for assessing the impact of the estimation quality of the parameter vector p on the system's closed-loop performance. Our goal is to determine acceptable ranges for the estimation errors. As with any estimation problem, the challenges are not only in determining the first and second-order statistics of the parameter estimation errors, but also in quantifying the impact of sensor noise on the estimate and the impact of the estimation accuracy on the closed-loop performance. The correspondence between estimation errors and performance metrics ultimately helps in selecting a desired estimation error threshold, and therefore establishing performance criteria for the estimation algorithm. In turn, the parameter estimation performance is affected by the user's choice of the excitation signal design during the data-collection phase and by the model structure selection. Ultimately, this sensitivity analysis provides guidance as to whether the current settings for estimation suffice to yield a suitably accurate model for the control purpose.

To generate a quantitative correspondence between the estimation errors and the closed-loop performance we take the following steps:

1) For designing the control algorithm, we use the same plant model M_R for control, but the parameters are offset by different values that mimic possible estimation errors δp. Hence the control model becomes $M_R([T_R,T_W],[u,T_E,Q_{R,int}],p_R+\delta p)$ as illustrated in Fig. 3.
2) We design the MPC in subsection III-A as an optimization algorithm with time-varying constraints on

T_R, input constraints on u, and time-varying energy prices. We also assume knowledge of the disturbances T_E and $Q_{R,int}$.

3) In subsection III-B, we simulate the closed-loop performance for a set of perturbations δp and for each value we compute the optimal value of the total energy cost. Constraint violation severity is also logged, since temperatures which are driven to their upper limits during peak-priced electricity hours are now liable, in the presence of unpredictable large values of δQ, to exceed their limits in the time between MPC input updates.
4) Using the data from the previous step we fit a linear mapping (in a Least Squares sense) between the energy cost and the parameters supplied to the MPC algorithm. We use this map to identify the most critical parameters and generate estimation error targets.

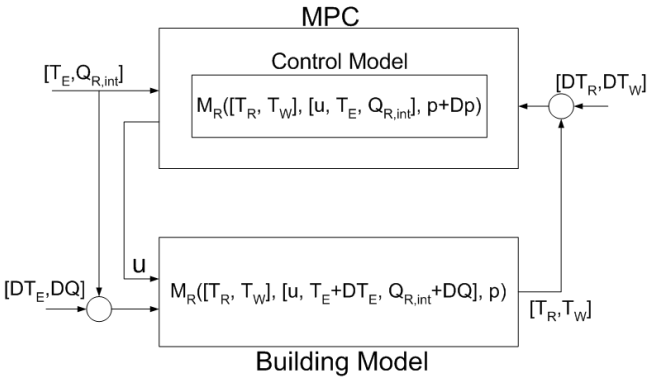

Fig. 3. Block diagram representation of MPC algorithm in closed-loop with room model M_R.

A. Model Predictive Control of Thermal Network

In this section we design a Model Predictive Control algorithm using the zone-level model $M_R([T_R, T_W], [u, T_E, Q_{R,int}], p_R)$ and we use it to determine the sensitivity of the optimal cost with respect to parameter p_R. We formulate the receding-horizon constrained problem and discuss the simulation results for the cases when disturbances T_E, uncontrolled-spaces temperatures, and internal loads $Q_{R,int}$ are not known exactly. We choose to use a standard MPC formulation rather than a so-called Robust MPC [5] since this requires constrained optimization of feedback policies, which is difficult when coupled with feedback linearization.

We use feedback-linearization [6] to redefine the control inputs as $u_i = C_{pa}\dot{m}_{sa,R_i}(T_{sa,R_i} - T_{R_i})$ which represent the thermal energy supplied to each room R_i. With this new input the model M_R, based on the (1), can be re-written as

$$\frac{d}{dt}T = A(p)T + B(p)u + D(p)T_E + Q_{R,int} \tag{4}$$

where T is the vector of all room and wall temperatures T_{R_i} and T_{w,S_i,S_j}, u is the vector of all supplied energies[2] u_i. In controlling the system (4) we want to minimize the total supplied energy cost. We denote the energy price $\alpha(t)(\frac{\$}{J})$ where the time-dependence captures the cost variation between high and low time periods. The cost function is:

$$J(M_R([T_R, T_W], [u, T_E, Q_{R,int}], p_R)) = \int_{t_0}^{t_f} [\textstyle\sum_i \alpha(t)u_i]\, dt \tag{5}$$

where the model used as the argument represents the control model as illustrated in Fig. 3. We impose input constraints and, to simplify the problem we assume that only cooling energy is required:

$$u_{min} \leq u_i(t) \leq 0,\ \forall t \in [t_0, t_f]. \tag{6}$$

where u_{min} is the minimum energy value (maximum cooling energy) that can be supplied to each zone R_i. By using feedback linearization the optimization problem can be formulated as a Linear Programming (LP) problem. In practice, hard constraints on $\dot{m}_{sa}$ and T_{sa,R_i} are present in which case one would have a non-convex optimization problem in order to handle them directly. In addition to input constraints, we have zone space temperature constraints imposed by practical implementations. During occupied hours the temperature is constrained to be within a range centered around a thermostat setting, whereas during unoccupied hours, these constraints are relaxed to minimize energy consumption. The constraints are illustrated by the dashed line in Fig. 4(d) and they can be written as:

$$T_{R,min}(t) \leq T_{R_i}(t) \leq T_{R,max}(t),\ \forall t \in [t_0, t_f]. \tag{7}$$

where we assume the same lower and upper bounds in all zones area are known *a priori*.

The receding horizon optimization problem is formulated with the system, cost, input and state constraints as defined above. The problem is cast as an LP problem by discretizing[3] the system (4) and solving at each step k an optimization problem with variables $[u_{k|k}, \cdots, u_{k+N|k}]$; at time each time step k we apply only the input $u_{k|k}$ and then iterate at time $k+1$. For the control model we use as the plant model with perturbed parameters $M_R([T_R,\ T_W], [u,\ T_E,\ Q_{R,int}], p_R + \delta p)$ and apply the generated optimal control inputs to the plant model $M_R, ([T_R, T_W], [u, T_E + \delta T_E, Q_{R,int} + \delta Q], p_R)$. The temperature δT_W and load δQ disturbances, combined with time elapsed between two consecutive control updates, may result in constraints infringement; i.e. the set

$$C_T \stackrel{\triangle}{=} \{t : T_{R,i}(t) < T_{R,min}(t) \text{ or } T_{R,i}(t) > T_{R,max}(t)\} \tag{8}$$

has non-zero measure. This is also the case when the control model parameter perturbations $\delta p = 0$. One could design a robust MPC which could use the upper bounds for $\|\delta T_E\|$ and $\|\delta Q\|$ and therefore use the model $M_R([T_R, T_W], [u, T_E + \delta T_E, Q_{R,int} + \delta Q], p_R + \delta p)$ to guarantee that the constraints (7) are met at all discrete steps k. However, we regard the constraints (7) as *soft* constraints–they are selected as a band centered around a thermostat setting–and we choose

[2]We use the same notation for the control input as in Section II where the input consisted of $\dot{m}_{sa}$ and T_{sa,S_i}.

[3]We use the same notation for the discrete system variables and cost as for the continuous-time system

instead to allow such infringements. For easier reference we denote the optimal cost (associated with the indicated control model):

$$J^\star(M_R, T_E, Q_{R,int}, p_R) = \min_u J(M_R([T_R, T_W], [u, T_E, Q_{R,int}], p_R). \quad (9)$$

We also denote the set $C_T(M_R, T_E, Q_{R,int}, p_R)$ to be the set in (8) associated with the optimal solution corresponding to the control model $M_R([T_R, T_W], [u, T_E, Q_{R,int}], p_R)$ and building model $M_R([T_R, T_W], [u, T_E + \delta T_E, Q_{R,int} + \delta Q], p_R)$. Likewise we defined the set $C_T(M_R, T_E, Q_{R,int}, p_R + \delta p)$ to be the set as in (8) associated with the optimal solution corresponding with the control model $M_R([T_R, T_W], [u, T_E, Q_{R,int}], p_R + \delta p)$ and the same building model.

B. Sensitivity Analysis

In this section we estimate the sensitivity of the optimal cost $J^\star(M_R, T_E, Q_{R,int}, p_R)$ with respect to parameter p_R. The goal is to determine estimation error targets for the parameter p_R. We first use the MPC algorithm developed in the previous section to generate a set of pairs $(p_i, J_i^\star)$ based on simulation results. Then we construct a linear map $\hat{J}^\star = \hat{J}^\star(p)$ and use it to determine the most critical parameters.

We perturb each of the parameters $p(i)$ and generate a set of parameter vectors $P = \{p_1, p_2, ...\}$, with $p_i = p_R + \delta p_i$; P represents a set of values that the estimation algorithm could potentially generate. The corresponding set of optimal costs $\{J_1^\star, J_2^\star, ...\}$ is generated for each value of the parameter, $J_i^\star = J^\star(M_R, T_E, Q_{R,int}, p_i)$, by simulating the MPC algorithm in closed-loop with the plant model $M_R, ([T_R, T_W], [u, T_E + \delta T_E, Q_{R,int} + \delta Q], p_R)$ as illustrated in Fig. 3. We use the values $(p_i, J_i^\star)$ to generate the affine map $\hat{J}^\star(p)$

$$\hat{J}^\star(p) = c_0 + c_w h_w + c_{gr} h_{gr} + c_{cei} h_{cei} + c_{hC} \frac{h_w}{C_w} + c_{RC} \frac{1}{R_w C_w} \quad (10)$$

where all coefficients c are calculated based on Least Squares approximation. The average percent error of the optimal cost approximation is less than 2%. The coefficients represent the sensitivity of the approximated cost with respect to the various parameters. Based on the relative values of these coefficients we conclude that h_{gr} and h_{ceil} are the most critical parameters (their coefficients are at least an order of magnitude higher than the rest of the coefficients). Figure 5 illustrates the dependency of closed-loop energy cost $J^\star(M_R, T_E, Q_{R,int}, p_R + \delta p)$ and constraint infringement time $C_T(M_R, T_E, Q_{R,int}, p_R + \delta p)$ on δh_{gr} and δh_{cei}. For a qualitative analysis of the influence of these two parameters on the two performance metrics we plot two optimal solutions in 4(c) and 4(d). We plot the optimal solutions for the case when the control model uses unperturbed parameters (red line) and perturbed parameters (blue line), with $\delta h_{gr} = 0.25 h_{gr}$, $\delta h_{cei} = -0.25 h_{cei}$ (corresponds to point (75%,125%) in Fig. 5). In both cases the building model is simulated with unknown disturbance components δT_E and δQ_R selected as normally distributed random variables. For easier reference, we denote the optimal solutions as $(x^\star_{\delta h=0}, u^\star_{\delta h=0}, J^\star_{\delta h=0})$ and $(x^\star_{\delta h\neq 0}, u^\star_{\delta h\neq 0}, J^\star_{\delta h\neq 0})$, respectively. Based on these plots we observe that $J^\star_{\delta h\neq 0} < J^\star_{\delta h=0}$ and this can be intuitively explained by comparing the two solutions on interval $[45, 60]h$ ($48h$ is the midnight of the second day of simulations). The discrepancies between the two solutions can be explained by analyzing the effect of T_E on the two control models, combined with their time constant changes. As δh_{gr} increases, the control model uses larger cooling energy values $u^\star_{\delta h\neq 0}$ earlier in order to meet the lower bound constraints that increases at $56h$. We observe that $x^\star_{\delta h=0}(56h)$ is closer to the lower bound constraint than $x^\star_{\delta h\neq 0}(56h)$. Because it predicts a larger energy transfer from the ground ($T_{gr} < T_{R_i}$), $x^\star_{\delta h\neq 0}$ uses less energy but infringes on the upper bound constraints on longer time intervals, hence $|C_T|$ (the measure of this set) associated with $x^\star_{\delta h\neq 0}$ is larger than $|C_T|$ associated with $x^\star_{\delta h=0}$. The perturbation δh_{cei} has the opposite effect on two metrics since $T_{cei} > T_{R_i}$.

Using the two sensitivity plots one can define levels of parameter errors that are both acceptable and achievable. We select this error target to be 10% which corresponds to a maximum 5% increase in energy cost and a maximum 100% increase in constraint violation time (most of the time the temperature increases by less than 0.5 (°C) beyond $T_{R,max}(t)$). The illustrated sensitivity magnitudes depend on the selected disturbance levels of this study.

IV. Parameter Estimation

In this section we use the estimation model $M_R([T_R, T_W], [u, T_E, Q_{R,int}], p_R)$ to estimate the parameter

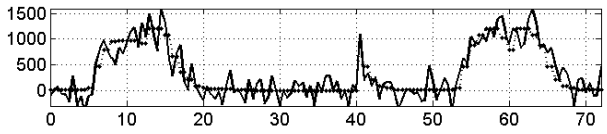

(a) Internal loads(W): actual (solid) and nominal (dashed) (x-axis:time (h)).

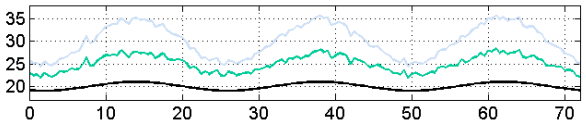

(b) Exogenous temperatures (°C): ceiling(blue), corridor (green) and ground (black) (x-axis:time (h)).

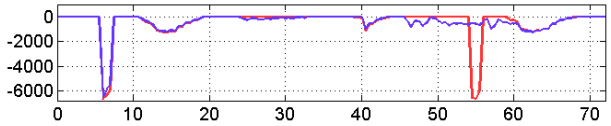

(c) Supplied thermal power (W): $u^\star_{\delta h=0}$ (red) and $u^\star_{\delta h\neq 0}$ (blue) (x-axis:time (h)).

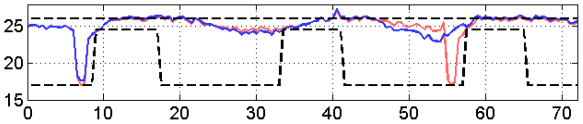

(d) Space temperatures (°C): $x^\star_{\delta h=0}$ (red) and $x^\star_{\delta h\neq 0}$ (blue) for one room (x-axis:time (h)).

Fig. 4. Plots of optimal inputs and states when control model parameters are the same as or different from model parameters.

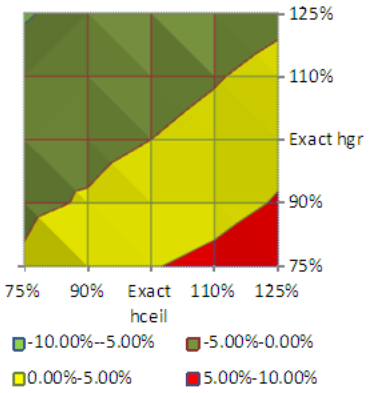

(a) Energy cost changes with respect to h_{gr} and h_{ceil}.

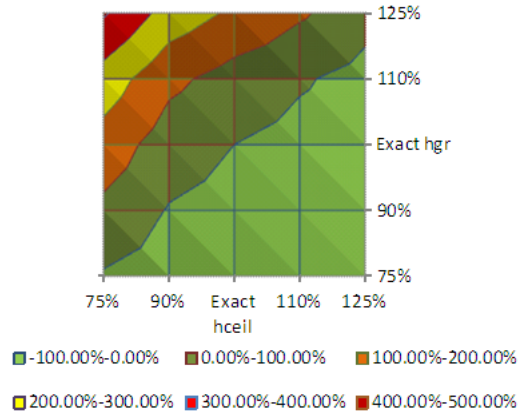

(b) Constraint infringement time with respect to h_g and h_{ceil}.

Fig. 5. Energy cost and constraint infringement metric variation with critical building model parameters; colored regions correspond to noted cost differences relative to the case when control model parameters are identical to plant model parameters.

vector p_R in the presence of sensor noise measurement and load disturbance, as illustrated in Fig. 6. Here we present the simulation results that are obtained with the Recursive

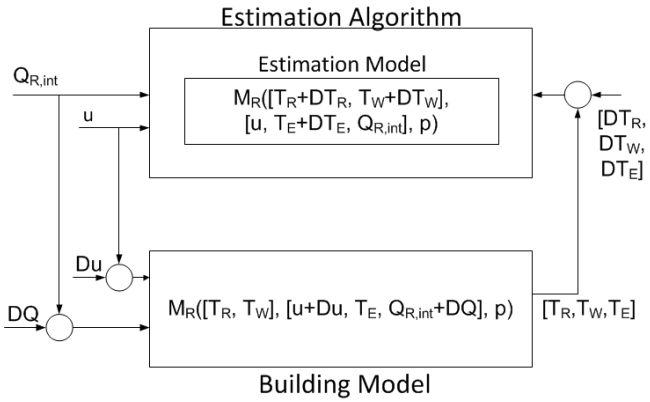

Fig. 6. Block diagram representation of the estimation algorithm and building model with simulated measurement noise and disturbances.

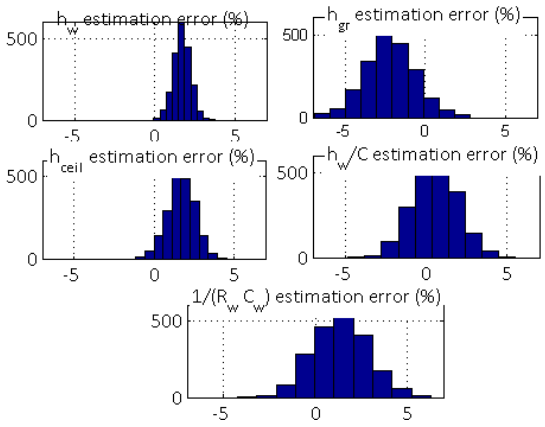

Fig. 7. Error distribution plots for parameter vector θ components based on Monte Carlo simulation results with sensor noise and load uncertainty (y-axis: count).

Least Squares algorithm. Other estimation approaches can be used such as : Finite-Time Method [7], variants of Least Squares (forgetting factors) [3]. We apply Recursive Least Squares to the discretized system of (3)

$$x_{k+1} = x_k + F_d(x_k, u_k) + G_d(x_k, T_{E,k})p_R + Q_{S,int,k} \tag{11}$$

for $k \in \{0, \cdots, N-1\}$, and note that the identifiability of the parameter p_R depends on the invertibility properties of the following matrix:

$$\begin{array}{l}[G_d(x_0, T_{E,0}) \ \cdots \ G_d(x_{N-1}, T_{E,N-1})] \\ \cdot[G_d(x_0, T_{E,0}) \ \cdots \ G_d(x_{N-1}, T_{E,N-1})]^T\end{array} \tag{12}$$

We make an additional assumption:

A7. For the simulation results $x_k = [T_{R,k}, T_{W,k}]$, the condition number of the matrix in (12) is minimum.

The relatively sparse structure of matrix G_d, mentioned in Section II, does not guarantee persistence of excitations, and therefore does not guarantee a unique solution for the estimate $\hat{p}_R$. In particular, the estimates of the most critical parameters $\hat{h}_{gr}$ and $\hat{h}_{cei}$ are not unique. This can be explained based on the original continuous-time equation (1), where the sum $(h_{gr} + h_{cei})$ multiplies each T_{R_i}, and each individual parameter multiplies one of the disturbances T_E. To illustrate the applicability of the proposed framework we apply the recursive least squares algorithm to simulation results generated during unoccupied time intervals and assume that the nominal load $Q_{R,int}$ is a constant that we also estimate. With the new notations $y_k = x_{k+1} - x_k - F_d(x_k, u_k)$ and $G_{d,k} = G_d(x_k, T_{E,k})$, the estimates are generated recursively as follows [3]:

$$\hat{p}_{R,k} = \hat{p}_{R,k-1} + K_k(y_k - G_{d,k}\hat{p}_{R,k-1}) \tag{13}$$

with the gain and state covariance matrices

$$\begin{array}{rcl} K_k & = & P_{k-1}G_{d,k}(I + G_{d,k}P_{k-1}G_{d,k}^T)^{-1} \\ P_k & = & (I - K_kG_{d,k})P_{k-1}. \end{array} \tag{14}$$

We assume the sensor measurement noise to be normally distributed with zero mean and standard deviations to be the

same as in [2]: space temperature noise $\delta T_{R,i}$ is $\pm 0.14(^{\circ}C)$; supply temperature noise $\delta T_{sa,R_i}$ is $\pm 0.14(^{\circ}C)$; supply air flow rate noise $\delta \dot{m}_{sa,R_i}$ is $\pm 0.0142(kg/s)$. The uncertain component of the load δQ_{R_i} was assumed to be a normally distributed random variable. With noise and load disturbances realized using these models, we conducted 2000 simulations and generated estimates whose error distributions are plotted in Fig. 7. Due to space limitations we do not include the time series simulation results. One notes that the two critical parameter's distributions have the largest mean (in absolute value), an expected consequence of the non-identifiability property as explained above. From the same plots, we also observe that the maximum estimation error for the critical parameters h_{gr} and h_{ceil} with the selected noise and uncertainties is less than the 10% target established in Section III.

V. CONCLUSIONS AND FUTURE WORK

A method for determining estimation-error targets for the parameters of a thermal network model of a building has been developed. These estimation error targets are established based on the sensitivity of closed-loop performance in the presence of control-model parameter errors. For these simulations we implemented an MPC algorithm that uses perturbed control model parameters, nominal values of loads, time-varying constraints and utility rates. After the estimation bounds were selected, we implemented standard estimation techniques to generate parameter values using the given model structure from (3) and its discretization (11) and excitation signal satisfying A.7. We conducted Monte-Carlo simulations with random sensor noise and load uncertainties and the results demonstrate that the estimation targets are met for the selected disturbance magnitudes subject to the persistence of excitation requirement.

The method presented in this paper can be extended to include bounds for parameter, state and load estimation errors based on their impact on closed-loop performance. Full-scale building data is now being used for parameter estimation and model validation. We plan on continuing this work also for the cases when not only the parameter vector but also the control model is different (reduced order) from the plant model.

VI. ACKNOWLEDGMENTS

The authors gratefully acknowledge the funding support offered by United Technologies Research Center for the analysis and simulation efforts. We are grateful for the funding provided by the Environmental Security Technology Certification Program for the Project EW-0938, Wireless Platform for Energy-Efficient Building Retrofits, supervised by Program Manager Dr. Jim Galvin. As part of this project we conducted the field functional tests and collected the sensor measurements that were used for the models and are now being used to extend the parameter estimation techniques to full-scale control experiments. In addition we acknowledge the suggestions and building information data received from the partners from Construction Engineering Research Laboratory, US Army Corps of Engineers, Champaign, IL. We also thank Sonja Glavaski and Miroslav Baric for suggestions provided to improve the manuscript.

REFERENCES

[1] "Energy Efficiency in Buildings: Transforming the Market", *World Business Council on Sustainable Development* (http://www.wbcsd.org), 2009.

[2] K. Lee and J.E. Braun,"Model-Based Demand-Limiting Control of Building Thermal Mass", *Building and Environment*, vol. 43, 2008, pp. 1633-1646.

[3] L. Ljung, *System Identification: Theory for the user*, Prentice Hall, NJ, 1999.

[4] F.C. McQuiston, J.D. Parker, J.D. Spitler, *Heating, Ventilating, and Air Conditioning, Analysis and Design*, Jon Wiley and Sons, Inc., 2005.

[5] P.J. Goulart, E.C. Kerrigan and J.M. Maciejowski, Optimization over state feedback policies for robust control with constraints, Automatica, vol. 42, 2006, pp. 523-533.

[6] H.K. Khalil, *Nonlinear Systems*, Prentice Hall, 1996.

[7] V. Adetola, M. Guay, "Finite-Time Parameter Estimation in Adaptive Control of Nonlinear Systems", *IEEE Transactions on Automatic Control*, vol. 53, 2008, pp. 807-811.

[8] T.L. McKinley and A.G. Alleyne, "Identification of Building Model Parameters and Loads using On-Site Data Logs", *Third National Conference of IBPSA-USA*, Berkely, CA USA, July 2008.

[9] S. Wang and X. Xu, "Simplified Building Model for Transient Thermal Performance Estimation using GA-based Parameter Identification", *International Journal of Thermal Sciences*, Vol. 45, pp. 419-432, 2006.

[10] K. Lee and J.E. Braun, "Development and Application of an Inverse Building Model for Demand Response in Small Commercial Buildings", *SimBuild 2004, IBPSA-USA National Conference*, Boulder, CO USA, August 2004.

[11] T. Dewson, B. Day, and A.D. Irving, "Least Square Parameter Estimation of a Reduced Order Thermal Model of an Experimental Building", *Building and Environment*, Vol. 28, pp. 127-137, 1993.

[12] Z. O'Neil, S. Narayanan, R. Brahme, "Model-Based Thermal Load Estimation in Buildings", SimBuild Conference, New York, Aug. 11-13, 2010.

[13] Website: *http://apps1.eere.energy.gov/buildings/energyplus*

[14] Website: *http://www.trnsys.com*

[15] S. Karatasou, M. Santamouris, and V. Geros, "Modeling and Predicting Building's Energy Use with Artificial Neural Networks: Methods and Results", *Energy and Buildings*, Vol. 38, pp. 949-958, 2006.

[16] M.J. Jiménez, H. Madsen, K.K. Andersen, "Identification of the Main Thermal Characteristics of Building Components using Matlab", *Building and Environment*, Vol. 43, pp. 170-180, 2008.

[17] T.Y. Chen and A.K. Athienitis, "Investigation of Practical Issues in Building Thermal Parameter Estimation", *Building and Environment*, Vol. 38, pp. 1027-1038, 2003.

[18] D. Gyalistras, M. Gwerder, F. Oldewurtel, C.N. Jones, M. Morari, B. Lehmann, K. Wirth, and V. Stauch, "Analysis of Energy Savings Potentials for Integrated Room Automation", *Clima-RHEVA World Congress*, Antalya, Turkey, 2010.

[19] M. Gwerder, D. Gyalistras, F. Oldewurtel, B. Lehmann, K. Wirth, V. Stauch, and J. Tödtli, "Potential Assessment of Rule-Based Control for Integrated Room Automation", *Clima-RHEVA World Congress*, Antalya, Turkey, 2010.